Author(s): Chatterjee, Rupa; Srivastava, Dinesh K.; Renk, Thorsten

Title: Triangular flow of thermal photons from an event-by-event hydrodynamic model for 2.76A TeV Pb + Pb collisions at the CERN Large Hadron Collider

Year: 2016

Version:

Triangular flow of thermal photons from an event-by-event hydrodynamic model for 2.76*A* TeV Pb + Pb collisions at the CERN Large Hadron Collider

Rupa Chatterjee,[1,*] Dinesh K. Srivastava,[1,†] and Thorsten Renk[2,3,‡]

[1]*Variable Energy Cyclotron Centre, 1/AF, Bidhan Nagar, Kolkata 700064, India*

[2]*Department of Physics, P.O. Box 35, FI-40014 University of Jyväskylä, Finland*

[3]*Helsinki Institute of Physics, P.O. Box 64, FI-00014 University of Helsinki, Finland*

We calculate the triangular flow parameter v_3 of thermal photons from an event-by-event ideal hydrodynamic model for 0–40% central collisions of Pb nuclei at $\sqrt{s_{NN}} = 2.76$ TeV at the CERN Large Hadron Collider. v_3 determined with respect to the participant plane (PP) is found to be nonzero and positive, and its p_T dependence is qualitatively similar to the elliptic flow parameter v_2(PP) of thermal photons in the range $1 \leqslant p_T \leqslant 6$ GeV/c. In the range $p_T \leqslant 3$ GeV/c, v_3(PP) is found to be about 50–75% of v_2(PP) and for $p_T > 3$ GeV/c the two anisotropy parameters become comparable. The value of v_3 is driven by local density fluctuations both directly via the creation of triangular geometry and indirectly via additional flow. As expected, the triangular flow parameter calculated with respect to the reaction plane v_3(RP) is found to be close to zero. We show that v_3(PP) strongly depends on the spatial size of fluctuations, especially in the higher p_T ($\geqslant 3$GeV/c) region where a larger value of σ results in a smaller v_3(PP). In addition, v_3(PP) is found to increase with the assumed formation time of the thermalized system.

I. INTRODUCTION

The observation of collective flow and its description in terms of fluid dynamics is a cornerstone in the contemporary understanding of the dynamics of ultrarelativistic heavy ion collisions in terms of the creation of thermalized quantum chromodynamics (QCD) matter. In many recent studies it has been shown that fluid dynamics utilizing event-by-event (E-by-E) fluctuating initial conditions (IC) [1–6] can be successfully used to explain the large bulk matter elliptic flow results for the most central collisions and also the significant triangular flow of charged particles at RHIC (Relativistic Heavy Ion Collider) and LHC (CERN Large Hadron Collider) energies [7–10], which were underestimated previously by hydrodynamics with smooth initial density distribution. E-by-E hydrodynamics with fluctuating IC also explains the hardening of charged particle spectra at larger p_T [1,11] and various structures observed in two-particle correlations [12], and it also has been used to constrain the viscosity-over-entropy ratio η/s from simultaneous measurement of elliptic and triangular flow coefficients [13].

The thermal emission of photons is sensitive to the initial hot and dense stage of the expanding system [14] and thus photons are considered as one of the probes suitable to study IC fluctuations. It has been shown that fluctuations in the initial density distribution lead to a significant enhancement in the production of thermal photons compared to a smooth initial density distribution in ideal hydrodynamic calculations [15]. Consequently a better agreement of the experimental direct photon spectrum was obtained in the region $p_T > 2$ GeV/c

[15] using the thermal contribution from the fluctuating IC. The enhancement due to IC fluctuations is found to be more pronounced for peripheral collisions than for central collisions and is less pronounced at LHC than at RHIC for similar centrality bins [16]. We have also shown that the elliptic flow calculated using the E-by-E hydrodynamics is substantially larger compared to the results from a smooth initial state averaged profile in the region $p_T > 2$ GeV/c [17], However, the results still fall below the experimental data, which is sometimes referred to as the photon "v_2 puzzle."

The success of fluid dynamics implies that the shape of the initial spatial geometry or more precisely the initial spatial anisotropy of the overlapping zone between the two colliding nuclei leads to azimuthally anisotropic pressure gradients. As a result, an anisotropic momentum distribution of the final state particles is observed. The momentum anisotropies of the emitted particles are usually quantified by expanding the invariant particle distribution in the transverse plane in terms of the Fourier decomposition:

$$\frac{dN}{d^2 p_T dY} = \frac{1}{2\pi} \frac{dN}{p_T dp_T dY} \times \left[1 + 2 \sum_{n=1}^{\infty} v_n(p_T) \cos n\left(\phi - \psi_n^{PP}\right) \right]. \quad (1)$$

In the equation above, v_n are called the anisotropic flow parameters, ϕ is azimuthal angle, and ψ_n^{PP} is the participant plane angle for coefficient v_n. The anisotropic flow parameters are estimated experimentally by considering event plane angle Ψ_n in place of the participant plane angle ψ_n^{PP} in the equation above. The elliptic flow parameter v_2 is a result of the almond shape of the initial geometry and is one of the key observables studied at the RHIC experiments [18]. The significantly large v_2 measured at RHIC is considered as a sign of collectivity in the produced system.

———————

*rupa@vecc.gov.in

†dinesh@vecc.gov.in

‡thorsten.i.renk@phys.jyu.fi

The observation of significant triangular flow anisotropy v_3 of hadrons is attributed to the collision geometry fluctuations leading to a potential initial triangularity of the overlapping zone [7]. This is different from the case of v_2 where the initial collision geometry already has an ellipsoid shape which dominates over the local fluctuations. As a result, when the anisotropic flow parameters are calculated by taking the final-state average over a large number of events, one finds large v_2 with respect to the reaction plane, whereas v_3 only takes a nonzero value when determined with respect to an E-by-E determined participant plane.

Triangular flow of photons is hence of particular interest as photons, unlike hadrons, are emitted from every phase of the expanding system and high p_T photons are emitted from the hot and dense early stages of system expansion, hence they can be expected to particularly probe the initial conditions. It is known that there are mechanisms which can potentially mimic photon v_2, such as photon production in the fragmentation of back-to-back jets, which in turn are correlated to the global reaction plane geometry by path-length-dependent attenuation. However, they can not easily mimic v_3 since a three-jet event is not typically triangular and at the same time correlated with the bulk matter triangularity. Thus, the photon v_3 would primarily be due to the hydrodynamic evolution of the system. The main motivation is to see whether there is a v_2 puzzle for photons only, or a v_3 puzzle as well, and the interpretation in both cases would be different. If there is a puzzle for v_2 only, we would conclude that there is an additional mechanism mimicking v_2. On the other hand if there is a puzzle in v_3 as well, we would conclude that we are missing something more essential in the dynamics of the fluid expansion. A recent study [19] has investigated triangular flow and higher flow harmonics of thermal photons from an E-by-E viscous hydrodynamic model with KLN and Glauber initial conditions and argued that this leads to a very sensitive measurement of viscosity.

There are three potential mechanisms by which the initial state might influence photon v_3: (a) fluctuating IC may lead to an overall triangular deformation of the matter distribution in the transverse plane which is mapped into a triangular flow patter. This is the mechanism leading to hadron v_3, but since the shape of the matter distribution can only be probed by late time dynamics when photon production above 1 GeV is suppressed by thermal factors, it is not evident that this mechanism also is dominant for electromagnetic emission (see Fig. 3 of [17]). (b) Fluctuating IC lead to irregularly shaped hotspots with copious photon production, and the early time evolution of such hotspots will likely lead to angular anisotropies in the photon emission. However, there is no obvious reason for this anisotropy to correlate with the hadronic v_3 event plane, and hence it can *a priori* be expected to average out in measurements unless a photon triangular event plane can be determined (which is, however, impossible in any real measurement due to the very limited number of high p_T photons in any given event). (c) Hotspots in the fluctuating IC lead indirectly, e.g., by development of additional radial flow, to a magnification of the photon v_3 generated by either a local or initial overall triangular deformation. Interpreting any result requires one to carefully disentangle these mechanisms.

In the present work we study the p_T dependent triangular flow of thermal photons from fluctuating IC in detail for 0–40% central collision of Pb nuclei at LHC and the dependence of v_3 on the fluctuation size parameter and the initial formation time of the system, and we interpret our findings in the light of the three mechanisms outlined above.

II. TRIANGULAR FLOW OF THERMAL PHOTONS FROM AN E-BY-E HYDRODYNAMIC FRAMEWORK

We use the E-by-E ideal hydrodynamic model framework developed in [1] to calculate the triangular flow anisotropy of thermal photons at LHC energy. This (2+1)-dimensional hydrodynamic model with fluctuating IC has been successfully used to reproduce the p_T spectra and elliptic flow of hadrons at RHIC [1]. It has also been used to calculate the spectra and elliptic flow of thermal photons at RHIC and at LHC energies [15–17].

A Monte Carlo Glauber model is used for the initial state. The standard two-parameter Woods-Saxon nuclear density profile is used to randomly distribute the nucleons into the two colliding nuclei. Two nucleons from different nuclei are assumed to collide when the relation $d^2 < \frac{\sigma_{NN}}{\pi^2}$ is satisfied, where d is the transverse distance between the colliding nucleons and σ_{NN} is the inelastic nucleon nucleon cross section. We take $\sigma_{NN} = 64$ mb at LHC.

An entropy initialized wounded nucleon (sWN) profile is used where the initial entropy density is distributed around the collision participants (wounded nucleons) using a two-dimensional Gaussian distribution function:

$$ s(x,y) = \frac{K}{2\pi\sigma^2} \sum_{i=1}^{N_{\mathrm{WN}}} \exp\left(-\frac{(x-x_i)^2 + (y-y_i)^2}{2\sigma^2} \right). \quad (2) $$

K is a constant in the equation above and the position of the ith nucleon in the transverse plane is denoted by (x_i, y_i). σ is the most important parameter in the above equation: it decides the granularity or the size of the initial density fluctuations. It is a free parameter and we use a default value of $\sigma = 0.4$ fm as before [1,15–17] for our calculation. We use an initial time $\tau_0 = 0.14$ fm/c [20] at LHC from the Eskola, Kajantie, Ruuskanen, Tuominen (EKRT) minijet saturation model [21] as default value. We later vary the values of both σ and τ_0 from their defaults to gain better understanding of v_3 and to check the sensitivity of our results to these two initial parameters.

The temperature at freeze-out is taken as 160 MeV, which reproduces the measured p_T spectra of charged pions at LHC. 170 MeV is considered as the transition temperature from the plasma phase to hadronic phase and we use a lattice based equation of state [22] for our calculation.

We use complete leading order (LO) plasma rates from [23] and hadronic rates from [24] to calculate the triangular flow of thermal photons from the fluctuating IC. Next-to-leading order (NLO) plasma rates from [25] are used to obtain the thermal photon spectra from smooth IC only because of numerical efficiency (note that the difference is small in the P_T region considered). The total thermal emission is obtained by integrating the emission rates ($R = EdN/d^3pd^4x$) over the

space-time history of the fireball as

$$E \frac{dN}{d^3 p} = \int d^4 x \, R(E^*(x), T(x)). \qquad (3)$$

Here $T(x)$ is the local temperature and $E^*(x) = p^\mu u_\mu(x)$, where p^μ is the four-momentum of the photons and u_μ is the local four-velocity of the flow field.

The triangular flow parameter v_3 is calculated with respect to the participant plane (which is considered a good approximation for the event plane [1]) using the relation

$$v_3^\gamma \{\mathrm{PP}\} = \left\langle \cos \left[3 \left(\phi - \psi_3^{\mathrm{PP}} \right) \right] \right\rangle_{\mathrm{events}}, \qquad (4)$$

where the participant plane (PP) angle is defined as [26]

$$\psi_3^{\mathrm{PP}} = \frac{1}{3} \arctan \frac{\int dx \, dy \, r^3 \sin(3\phi) \varepsilon(x, y, \tau_0)}{\int dx \, dy \, r^3 \cos(3\phi) \varepsilon(x, y, \tau_0)} + \pi/3. \qquad (5)$$

Here ε is the energy density, $r^2 = x^2 + y^2$, and ϕ is the azimuthal angle. The triangularity or the initial triangular eccentricity of the matter density is calculated using the relation

$$\epsilon_3 = - \frac{\int dx \, dy \, r^3 \cos \left[3 \left(\phi - \psi_3^{\mathrm{PP}} \right) \right] \varepsilon(x, y, \tau_0)}{\int dx dy \, r^3 \varepsilon(x, y, \tau_0)}. \qquad (6)$$

III. RESULTS

Thermal photon p_T spectra for 0–40% central collisions of Pb nuclei at $\sqrt{s_{\mathrm{NN}}} = 2.76$ TeV at LHC are shown in Fig. 1. Results from smooth IC (SIC) using complete LO plasma rates (blue dotted line) and NLO plasma rates (solid orange line) are compared. Here the smooth IC is obtained by taking the initial-state average of 10 000 random events, which essentially removes all the fluctuations in the initial density distribution. We see that the addition of NLO contribution to the complete
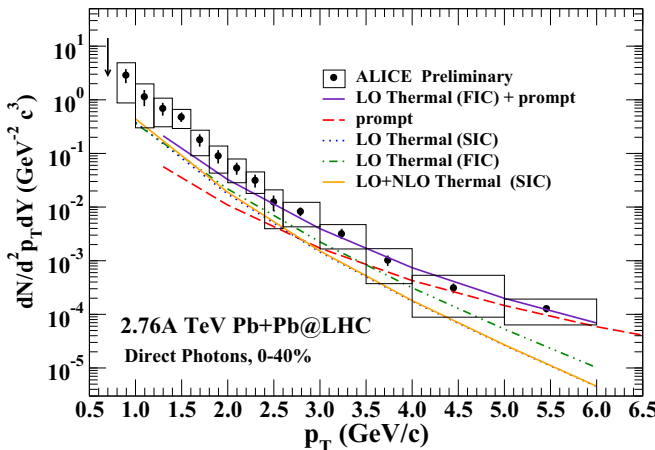

FIG. 1. Thermal photon p_T spectra from fluctuating IC (FIC) and smooth IC (SIC) considering complete leading order plasma rates [23] for 2.76 A TeV Pb + Pb collisions at LHC and for the 0–40% centrality bin. The p_T spectrum using next-to-leading order plasma rates [25] (for SIC only), ALICE direct photon data [28], and prompt photons from next-to-leading order pQCD calculations are also plotted for comparison.
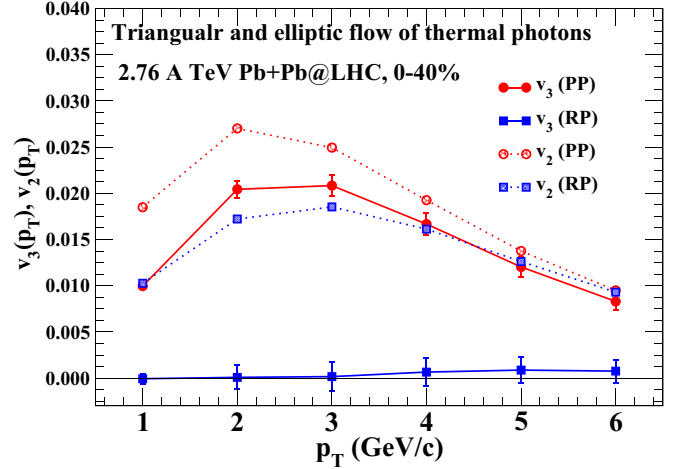

FIG. 2. Triangular and elliptic flow of thermal photons with respect to RP and PP for 0–40% central collisions of Pb nuclei at LHC and for $\sigma = 0.4$ fm.

LO rate increases the thermal photon production by 10–15% in the range $p_T < 2$ GeV/c, whereas for $p_T > 2$ GeV/c LO and NLO spectra look quite similar and fall on top of each other. This justifies our use of LO rates for the computation of v_2 and v_3 for numerical efficiency. We observe, however, that the additional NLO contribution to the thermal photon production is still not sufficient to match the experimental data in the range $p_T < 2$ GeV/c.

As shown before [16], thermal photons from fluctuating IC (FIC) along with prompt photons from NLO pQCD [27] calculation explain the direct photon p_T spectrum measured by ALICE [28] well in the region $p_T > 2$ GeV/c. The result from the fluctuating IC is obtained by taking the final-state average over the p_T spectra from a large number of random events.

Figure 2 shows triangular flow parameter v_3 of thermal photons as a function of p_T for 0–40% central collision of Pb nuclei at $\sqrt{s_{NN}} = 2.76$ TeV at LHC. The v_3 calculated with respect to the participant plane (red solid line, closed circles) as well as to the reaction plane (RP) (blue solid line, closed squares) are shown for $\sigma = 0.4$ fm. The elliptic flow parameters v_2(PP) and v_2(RP) calculated for the same centrality bin [17] are shown as well for comparison. The v_3 results are obtained by averaging over the triangular flow results from 400 random events and we also show the standard errors on both the v_3(PP) and v_3(RP).

We see that v_3(PP) for thermal photons is positive and significant compared to the the elliptic flow results calculated for the same centrality bin in the region $1 \leqslant p_T \leqslant 6$ GeV/c. At $p_T = 1$ GeV/c, the difference between v_3(PP) and v_2(PP) is maximum and v_3(PP) is almost half of the value of v_2(PP) at this p_T. The difference reduces more and more towards higher values of p_T. v_3(PP) is about 80% of the value of v_2(PP) at $p_T = 3$ GeV/c, and at $p_T = 5$ GeV/c the difference between the two results is about 10–15%.

When calculated with respect to the reaction plane, triangular flow from individual events is found to be both positive and negative. As expected, the averaged v_3(RP) is zero within errors, as shown in Fig. 2.

In order to understand the individual effects of initial geometry and local fluctuations on the triangular flow results better, we study v_3 of individual events by keeping the the number of wounded nucleons (N_{WN}) fixed. We take $N_{WN} = 200$ and generate random events having different triangular flow eccentricity. The number of binary collisions N_{coll} also varies in a wide range in those events. If the strength of photon v_3 is determined chiefly by the initial global triangular deformation ϵ_3, we expect to see that events with the largest ϵ_3 also show the largest v_3. If this is not observed, the mechanism generating v_3 from fluctuations is more intricate.

The variation of average transverse flow velocity with proper time for three different events with fixed N_{WN} is shown in upper panel of Figure 3. The N_{coll} values for events 1, 2, and 3 are 537, 611, and 724 respectively and the initial triangular eccentricities of the events are 0.122, 0.325, and 0.177 respectively. We observe that the average transverse flow velocity with time is largest for event 3; the event with maximum N_{coll} and for which $\langle v_T \rangle$ is smallest is event 1.

The v_3 calculated with respect to the PP for the three events is shown in lower panel of Fig. 3. Interestingly, the largest v_3 is *not* obtained for the largest ϵ_3 Instead, v_3 shows ordering

FIG. 4. Triangular flow of thermal photons for 0–40% central collisions of Pb nuclei at LHC and for size parameter $\sigma = 0.4$ and 0.8 fm.
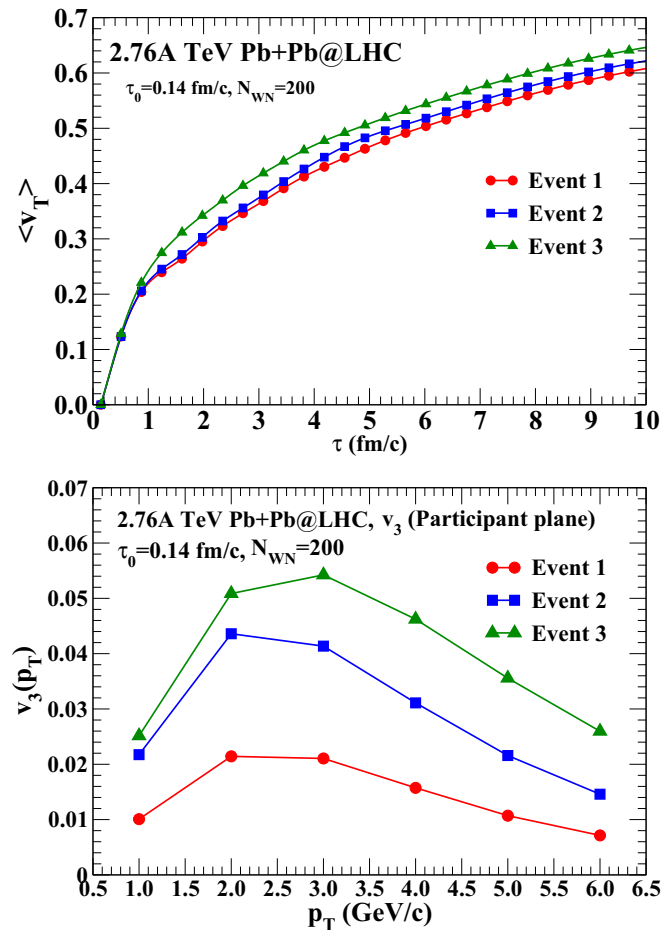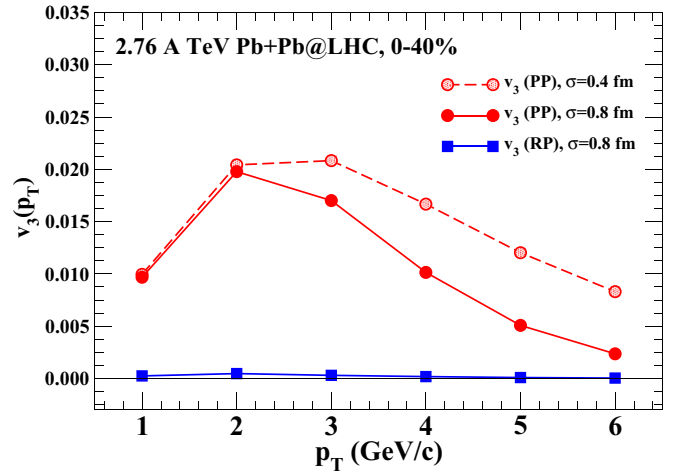

FIG. 3. Upper panel: Average transverse flow velocities for different events with fixed number of wounded nucleons. Lower panel: v_3(PP) for the same events.

similar to the average transverse flow velocity where v_3(PP) is largest for event 3 and is smallest for event 1, although the triangular eccentricity is maximum for event 2. This argues that indirect effects of fluctuations, such as the buildup of a strong flow field, contribute significantly to the observed result beyond the initial triangular eccentricity. It has been shown in Ref. [29] that, for events with same number of participants, the average p_T fluctuates in those events due to the fluctuations in the initial state and the flow velocities.

Let us now investigate the systematics for variations of the initial-state parameters. The fluctuation size scale σ is an important parameter as both the geometry and the overall strength of photon emission are strongly sensitive to its value. The initial density distribution becomes smoother for larger values of size parameter, and in an earlier study [17] we have shown that the elliptic flow parameter for $\sigma = 1.0$ fm is quite similar to the elliptic flow parameter calculated using a smooth initial-state averaged IC. Thus, it is crucial to also study the dependence of photon v_3 on the value of σ. Figure 4 shows v_3(PP) and v_3(RP) as a function of p_T for 0–40% central collisions of Pb nuclei at $\sqrt{s_{NN}} = 2.76$ TeV at LHC and for two different σ values. As shown in the figure, the value of v_3(PP) for $\sigma = 0.4$ fm (red dashed line, open circles) is close to the v_3(PP) results for $\sigma = 0.8$ fm (red solid line, closed circles) in the lower p_T ($\leqslant 2$ GeV/c) region. However, for $p_T > 2$ GeV/c, v_3(PP) is smaller for the larger value of σ, and with increasing p_T the v_3(PP) for $\sigma = 0.8$ fm falls sharply compared to the flow result for $\sigma = 0.4$ fm.

This is consistent with our earlier observations: The presence of the local fluctuations or the hotspots in the IC results in stronger radial flow velocity, which allows us to probe the initial geometry more efficiently and we see larger v_3 for the smaller value of σ.

One can expect even larger v_3(PP) (than the results shown in Fig. 2) when σ is smaller than 0.4 fm. However, the flow anisotropy calculation become numerically expensive for smaller values of σ and thus we cannot yet show reliable results for $\sigma < 0.4$ fm.
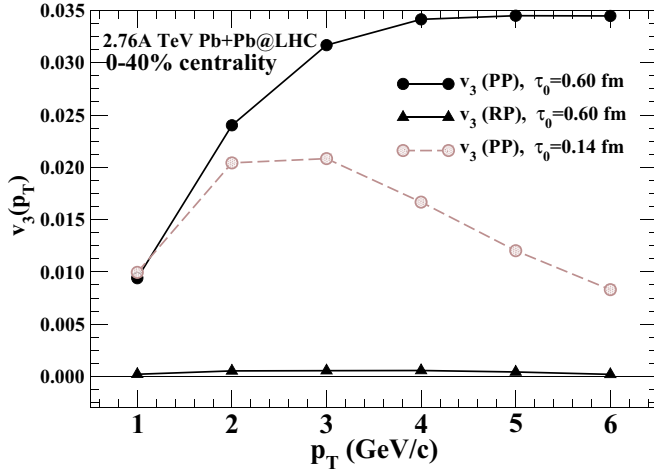
FIG. 5. Triangular flow of thermal photons for 0–40% central collisions of Pb nuclei at LHC and for size parameter $\sigma = 0.4$ and at τ_0 values 0.14 and 0.6 fm/c.

As expected, the triangular flow parameter calculated with respect to the RP does not depend on the value of σ and v_3(RP) close to zero for $\sigma = 0.8$ fm (shown by black solid line, closed triangles).

Next we study the dependence of the triangular flow parameter on the initial formation time τ_0 of the plasma. All the v_3 results shown till now were calculated for a very small $\tau_0 = 0.14$ fm, which is taken from the EKRT model [21] for most-central collisions of Pb nuclei at LHC. Now the formation time of the plasma can be larger for peripheral collisions than for central collisions [16]. As we do not have the formation time at LHC for the 0–40% centrality bin from the EKRT model, we choose a sufficiently large $\tau_0 = 0.6$ fm/c to start the hydrodynamic calculation in order to see the dependence of v_3 on the initial formation time of the plasma. It is quite well known that photon spectra depend strongly on the value of τ_0 [16], where the spectra fall sharply for larger τ_0.

Figure 5 shows v_3(PP) as a function of p_T for τ_0 values 0.14 and 0.6 fm/c and for $\sigma = 0.4$ fm. It should be noted that the triangular flow parameter for two different τ_0 values is calculated by keeping the total entropy per unit rapidity of the system fixed.

The v_3(PP) for larger τ_0 rises rapidly compared to the flow parameter calculated using smaller τ_0 in the region $p_T \leqslant 3$ GeV/c. For $p_T > 3$ GeV/c, v_3 for $\tau_0 = 0.6$ fm/c does not change significantly with p_T and becomes constant. This is in contrast to the v_3 for $\tau_0 = 0.14$ fm/c which drops with increasing p_T. The high p_T photons are emitted early when the presence of local fluctuations in the IC is strong. However, these photons do not contribute significantly to the v_3 result and the small values of transverse flow velocity in the initial stage brings the v_3 down for $p_T > 3$ GeV/c when a smaller τ_0 is considered. For $\tau_0 = 0.6$ fm/c, a large fraction of these high p_T photons are not included in the calculation, and as a result we get much larger v_3 [30]. We see that when the azimuthally isotropic prompt contribution (which dilutes the photon anisotropic flow at larger p_T) remains the same, the total v_3 from thermal and prompt contributions is slightly larger for $\tau_0 = 0.14$ fm than for $\tau_0 = 0.60$ fm.

Figure 5 explicitly shows that the eccentricity of initial hotspots does not contribute to photon v_3 directly as expected; only photons emitted somewhat later when flow had time to develop carry significant v_3. We can combine this with with Fig. 3 to conclude that, while a nonzero ϵ_3 is needed to find any triangular flow, the most important effect of initial fluctuations on thermal photon v_3 is indirect, i.e., the modification of the radial flow pattern which can transform even a small initial ϵ_3 into a large v_3.

IV. SUMMARY AND CONCLUSIONS

We calculate the triangular flow anisotropy of thermal photons from an E-by-E ideal hydrodynamic model. The complete leading order plasma rates and state-of-the-art hadronic rates are used to calculate v_3 at LHC using suitable initial and final conditions. We show that the inclusion of NLO plasma rate to the complete LO rates does not change the spectra results significantly for $p_T \geqslant 2$ GeV/c.

The flow parameter v_3 as a function of p_T is calculated with respect to the reaction plane and participant plane for $2.76A$ TeV Pb + Pb collisions at LHC and for 0–40% central collisions. The value of v_3(PP) at $p_T = 1$ GeV/c is found to be about 50% smaller than the v_2(PP) calculated using same initial and final conditions. However, the two results become comparable for $p_T > 3$ GeV/c. The triangular flow anisotropy calculated with respect to the RP is close to zero.

The v_3(PP) calculated using $\sigma = 0.8$ fm is found to be similar to v_3(PP) for $\sigma = 0.4$ fm in the region $p_T \leqslant 2$ GeV/c. For larger p_T, however, the v_3 for larger σ is relatively smaller in magnitude. We see the variation of average transverse flow velocity with proper time and v_3(PP) as a function of p_T as well for different events with same number of wounded nucleons. This is done in order to understand the role of $\langle v_T \rangle$ and ϵ_3 in determining the triangular flow anisotropy parameter better. v_3 as a function of p_T for two different values of initial formation time are also compared. A larger τ_0 results in a much larger v_3 compared to the result calculated using a smaller τ_0.

We find that photon v_3 probes the initial state geometry in an indirect way via the generation of additional transverse flow. The sensitivity to the fluctuation size scale as well as to the equilibration time offers useful constraints for a dynamical modeling of the pre-equilibrium phase.

[1] H. Holopainen, H. Niemi, and K. J. Eskola, Phys. Rev. C **83**, 034901 (2011).

[2] B. Schenke, P. Tribedy, and R. Venugopalan, Phys. Rev. Lett. **108**, 252301 (2012).

[3] U. Heinz, Z. Qiu, and C. Shen, Phys. Rev. C **87**, 034913 (2013).

[4] C. E. Coleman-Smith, H. Petersen, and R. L. Wolpert, J. Phys. G **40**, 095103 (2013).

[5] P. Sorensen, J. Phys. G **37**, 094011 (2010).

[6] J. Takahashi, B. M. Tavares, W. L. Qian, R. Andrade, F. Grassi, Y. Hama, T. Kodama, and N. Xu, Phys. Rev. Lett. **103**, 242301 (2009).

[7] B. Alver and G. Roland, Phys. Rev. C **81**, 054905 (2010).

[8] A. Adare *et al.* (PHENIX Collaboration), Phys. Rev. Lett. **107**, 252301 (2011).

[9] Z. Qiu, C. Shen, and U. Heinz, Phys. Lett. B **707**, 151 (2012).

[10] G. Aad *et al.* (ATLAS Collaboration), Phys. Rev. C **86**, 014907 (2012).

[11] Y. Hama, T. Kodama, and O. Socolowski, Braz. J. Phys. **35**, 24 (2005).

[12] R. Andrade, F. Grassi, Y. Hama, T. Kodama, and O. Socolowski, Phys. Rev. Lett. **97**, 202302 (2006); R. P. G. Andrade, F. Grassi, Y. Hama, T. Kodama, and W. L. Qian, *ibid.* **101**, 112301 (2008).

[13] B. Schenke, S. Jeon, and C. Gale, Phys. Rev. Lett. **106**, 042301 (2011).

[14] P. V. Ruuskanen, Nucl. Phys. A **544**, 169 (1992) and references therein; D. K. Srivastava, J. Phys. G **35**, 104026 (2008).

[15] R. Chatterjee, H. Holopainen, T. Renk, and K. J. Eskola, Phys. Rev. C **83**, 054908 (2011); J. Phys. G: Nucl. Part. Phys. **38**, 124136 (2011).

[16] R. Chatterjee, H. Holopainen, T. Renk, and K. J. Eskola, Phys. Rev. C **85**, 064910 (2012); Nucl. Phys. A **910**, 207 (2013).

[17] R. Chatterjee, H. Holopainen, I. Helenius, T. Renk, and K. J. Eskola, Phys. Rev. C **88**, 034901 (2013).

[18] C. Adler *et al.* (STAR Collaboration), Phys. Rev. Lett. **87**, 182301 (2001); **89**, 132301 (2002); **90**, 032301 (2003); S. S. Adler *et al.* (PHENIX Collaboration), *ibid.* **91**, 182301 (2003).

[19] C. Shen, U. W. Heinz, J.-F. Paquet, I. Kozlov, and C. Gale, Phys. Rev. C **91**, 024908 (2015).

[20] R. Paatelainen, K. J. Eskola, H. Holopainen, and K. Tuominen, Phys. Rev. C **87**, 044904 (2013).

[21] K. J. Eskola, K. Kajantie, P. V. Ruuskanen, and K. Tuominen, Nucl. Phys. B **570**, 379 (2000).

[22] M. Laine and Y. Schroder, Phys. Rev. D **73**, 085009 (2006).

[23] P. Arnold, G. D. Moore, and L. G. Yaffe, J. High Energy Phys. 12 (2001) 009.

[24] S. Turbide, R. Rapp, and C. Gale, Phys. Rev. C **69**, 014903 (2004).

[25] J. Ghiglieri, J. Hong, A. Kurkela, E. Lu, G. D. Moore, and D. Teaney, J. High Energy Phys. 05 (2013) 010.

[26] H. Niemi, G. S. Denicol, H. Holopainen, and P. Huovinen, Phys. Rev. C **87**, 054901 (2013).

[27] I. Helenius, H. Paukkunen, and K. J. Eskola, J. High Energy Phys. 05 (2013) 030.

[28] M. Wilde (ALICE Collaboration), Nucl. Phys. A **904**, 573c (2013).

[29] P. Bozek and W. Broniowski, Phys. Rev. C **85**, 044910 (2012).

[30] R. Chatterjee and D. K. Srivastava, Phys. Rev. C **79**, 021901(R) (2009); Nucl. Phys. A **830**, 503c (2009).